

# Chromophore-Labeled Quinoxaline Derivatives as Efficient Electroluminescent Materials

K. R. Justin Thomas,<sup>†</sup> Marappan Velusamy,<sup>†</sup> Jiann T. Lin,<sup>\*,†,‡</sup> Chang-Hao Chuen,<sup>†</sup> and Yu-Tai Tao<sup>\*,†</sup>

*Institute of Chemistry, Academia Sinica, 115 Nankang, Taipei, Taiwan, and  
Department of Chemistry, National Central University, 320 Chungli, Taiwan*

*Received December 31, 2004. Revised Manuscript Received February 2, 2005*

Electroluminescent materials comprising quinoxaline, triarylamine, and fluorophores such as carbazole, pyrene, and fluorene were prepared by using a key step involving a Pd-catalyzed C–N coupling reaction. Chromophores were embedded both at quinoxaline and triarylamine units, and their influence on photophysical and thermal properties was investigated. Quinoxalines possessing more electron-donating amines exhibit lower fluorescence quantum efficiency and the photoluminescence (PL) is severely affected by the polarity of the solvent used for measurement. Bulky and rigid aromatic groups such as pyrene and carbazole enhance the glass transition temperature of the derivatives. Oxidation potential of the triarylamine was easily tuned by the aromatic substituents while retaining the reduction potential of the quinoxaline segment. This provides us a method for tuning the photophysical and thermal properties maintaining the energy levels of the dipolar compounds. The electroluminescent devices fabricated using these materials as hole-transporters and emitters led to intense light emission. The emission color is green and corresponds well with the film PL of the material used.

## Introduction

Semiconducting organic and organometallic materials have attracted wide attention in the past decade owing to their potential application in fiber-optics,<sup>1</sup> photovoltaics,<sup>2</sup> and electroluminescent devices.<sup>3</sup> Organic light-emitting diodes (OLEDs) typically contain three layers of amorphous organic/organometallic materials to serve the hole-transport, electron-transport, and emission requirements of the device. Multifunctional molecules are designed, synthesized, and evaluated by many groups in an attempt to eliminate the cumbersome stepwise deposition procedure.<sup>4–8</sup> Both conjugated and nonconjugated dipolar compounds have been prepared for this purpose. In addition to the stabilization of both cations

and anions, which is essential to the robustness of the material during the transport of the holes and electrons, the donor–acceptor type derivatives give red-shifted emission, though with low quantum yield due to the dipolar quenching. These materials also crystallize readily due to large dipole

\* To whom correspondence should be addressed. Fax: 886-2-27831237. E-mail: jtlin@chem.sinica.edu.tw.

<sup>†</sup> Academia Sinica.

<sup>‡</sup> National Central University.

- (1) (a) Samyn, C.; Verbiest, T.; Persoons, A. *Macromol. Rapid. Commun.* **2000**, *21*, 1. (b) Delaire, J. A.; Nakatani, K. *Chem. Rev.* **2000**, *100*, 1817. (c) Kajzar, F.; Lee, K.-S.; Jen, A. K.-J. *Adv. Polym. Sci.* **2003**, *161*, 1.
- (2) (a) Gross, R.; Leach, M.; Bauen, A. *Environ. Int.* **2003**, *29*, 105. (b) Gregg, B. A. *ACS Symp. Ser.* **2003**, *844*, 243. (c) Hagfeldt, A.; Grätzel, M. *Acc. Chem. Res.* **2000**, *33*, 269. (d) Peumans, P.; Yakimov, A.; Forrest, S. R. *J. Appl. Phys.* **2003**, *93*, 3693. (e) Dimitrakopoulos, C. D.; Malenfant, P. R. L. *Adv. Mater.* **2002**, *14*, 99.
- (3) (a) Sheats, J. R.; Antoniadis, H.; Hueschen, M.; Leonard, W.; Miller, J.; Moon, R.; Roitman, D.; Stocking, A. *Science* **1996**, *273*, 884. (b) Gross, M.; Muller, D. C.; Nothofer, H. G.; Scherf, U.; Neher, D.; Brauchle, C.; Meerholz, K. *Nature* **2000**, *405*, 661. (c) Hung, L. S.; Chen, C. H. *Mater. Sci. Eng. Rep.* **2002**, *39*, 143. (d) Shim, H. K.; Jin, J. I. *Adv. Polym. Sci.* **2002**, *158*, 193. (e) Muller, C. D.; Falcou, A.; Reckefuss, N.; Rojahn, M.; Wiederhorn, V.; Rudati, P.; Frohne, H.; Nuyken, O.; Becker, H.; Meerholz, K. *Nature* **2003**, *421*, 829. (f) Slinker, J.; Bernards, D.; Houston, P. L.; Abruna, H. D.; Bernhard, S.; Malliaras, G. G. *Chem. Commun.* **2003**, 2392. (g) Akcelrud, L. *Prog. Polym. Sci.* **2003**, *28*, 875. (h) Mitschke, U.; Bäuerle, P. *J. Mater. Chem.* **2000**, *10*, 1471. (i) Segura, J. L. *Acta Polym.* **1998**, *49*, 319.

- (4) (a) Shu, C. F.; Dodda, R.; Wu, F. I.; Liu, M. S.; Jen, A. K. Y. *Macromolecules* **2003**, *36*, 6698. (b) Guan, M.; Bian, Z. Q.; Zhou, Y. F.; Li, F. Y.; Li, Z. J.; Huang, C. H. *Chem. Commun.* **2003**, 2708. (c) Chan, L. H.; Lee, R. H.; Hsieh, C. F.; Yeh, H. C.; Chen, C. T. *J. Am. Chem. Soc.* **2002**, *124*, 6469. (d) Paik, K. L.; Baek, N. S.; Kim, H. K.; Lee, J.-H.; Lee, Y. *Macromolecules*, **2002**, *35*, 6782. (e) Yeh, H. C.; Lee, R. H.; Chan, L. H.; Lin, T. Y. J.; Chen, C. T.; Balasubramanian, E.; Tao, Y.-T. *Chem. Mater.* **2001**, *13*, 2788. (f) Mochizuki, H.; Hasui, T.; Kawamoto, M.; Shiono, T.; Ikeda, T.; Adachi, C.; Taniguchi, Y.; Shirota, Y. *Chem. Commun.* **2000**, 1923. (g) Tamoto, N.; Adachi, C.; Nagai, K. *Chem. Mater.* **1997**, *9*, 1077. (h) Mochizuki, H.; Hasui, T.; Kawamoto, M.; Ikeda, T.; Adachi, C.; Taniguchi, Y.; Shirota, Y. *Macromolecules* **2003**, *36*, 3457. (i) Peng, Z. H.; Bao, Z. N.; Galvin, M. E. *Chem. Mater.* **1998**, *10*, 2086. (j) Jiang, X. Z.; Register, R. A.; Killeen, K. A.; Thompson, M. E.; Pschenitzka, F.; Heibner, T. R.; Sturm, J. C. *J. Appl. Phys.* **2002**, *91*, 6717.
- (5) (a) Justin Thomas, K. R.; Lin, J. T.; Tao, Y.-T.; Chien, C. H. *Chem. Mater.* **2002**, *14*, 2796. (b) Justin Thomas, K. R.; Lin, J. T.; Tao, Y.-T.; Chien, C. H. *J. Mater. Chem.* **2002**, *12*, 3516. (c) Justin Thomas, K. R.; Lin, J. T.; Tao, Y.-T.; Chien, C. H. *Chem. Mater.* **2002**, *14*, 3852. (d) Wang, P. F.; Xie, Z. Y.; Wong, O. Y.; Lee, C. S.; Wong, N. B.; Hung, L. S.; Lee, S. T. *Chem. Commun.* **2002**, 1404. (e) Wang, P. F.; Xie, Z. Y.; Hong, Z. R.; Tang, J. X.; Wong, O. Y.; Lee, C. S.; Wong, N. B.; Lee, S. T. *J. Mater. Chem.* **2003**, *13*, 1894.
- (6) (a) Tao, Y.-T.; Chuen, C.-H.; Ko, C.-W.; Peng, J.-W. *Chem. Mater.* **2002**, *14*, 4256. (b) Wang, Y. Z.; Epstein, A. J. *Acc. Chem. Res.* **1999**, *32*, 217 and references therein. (c) Jenekhe, S. A.; Lu, L. D.; Alam, M. M. *Macromolecules* **2001**, *34*, 7315.
- (7) (a) Kim, J. H.; Lee, H. *Chem. Mater.* **2002**, *14*, 2270. (b) Xie, Z. Y.; Hung, L. S.; Lee, S. T. *Appl. Phys. Lett.* **2001**, *79*, 1048. (c) Zhang, X. H.; Chen, B. J.; Lin, X. Q.; Wong, O. Y.; Lee, C. S.; Kwong, H. L.; Lee, S. T.; Wu, S. K. *Chem. Mater.* **2001**, *13*, 1565.
- (8) (a) Shirota, Y.; Kinoshita, M.; Noda, T.; Okumoto, K.; Ohara, T. *J. Am. Chem. Soc.* **2000**, *122*, 11021. (b) Doi, H.; Kinoshita, M.; Okumoto, K.; Shirota, Y. *Chem. Mater.* **2003**, *15*, 1080. (c) Mutaguchi, D.; Okumoto, K.; Ohsedo, Y.; Moriwaki, K.; Shirota, Y. *Org. Electron.* **2003**, *4*, 49.

moment. Crystallinity affects the homogeneity of the layered material and leads to grain boundaries that are detrimental to the function of OLEDs.

We have directed our research efforts to eliminate the above-mentioned drawbacks by designing quinoxaline derivatives containing triarylamine and another chromophore.<sup>5a,5b</sup> Quinoxalines are known to function as electron-transporting materials.<sup>5d,5e</sup> Our intention on incorporating triarylamine in the structure is to impart the hole-transport function. We have demonstrated earlier that the dyads derived from quinoxaline and triarylamine exhibit improved balance of hole and electron mobility in the molecular layer.<sup>5a</sup> We believe that the chromophores such as pyrene and fluorene will enhance the emission quantum yield of the compounds while the carbazole and pyrene will be beneficial to the thermal stability and glass transition temperature.<sup>9</sup> In this report, we conduct systematic exploration of quinoxaline compounds tethered with fluorene and/or carbazole moieties for the use in OLEDs. Two quinoxaline analogues appeared in an earlier report of us.<sup>5c</sup>

## Experimental Section

**General Information.** Unless otherwise specified, all reactions and manipulations were performed under nitrogen atmosphere using standard Schlenk techniques. All chromatographic separations were carried out on silica gel (60 M, 230–400 mesh). Dichloromethane and toluene were distilled from calcium hydride and Na/benzophenone respectively under nitrogen atmosphere. <sup>1</sup>H NMR spectra were recorded on a Bruker AC300 spectrometer. Fast-atom bombardment (FAB) mass spectra were collected on a JMS-700 double-focusing mass spectrometer (JEOL, Tokyo, Japan) with a resolution of 8000 (5% valley definition). For FAB mass spectra, the source accelerating voltage was operated at 10 kV with Xe gun, using 3-nitrobenzyl alcohol as matrix. Elemental analyses were performed on a Perkin-Elmer 2400 CHN analyzer. Electronic absorption spectra were measured on a Cary 50 Probe UV–vis spectrometer. Emission spectra were recorded by a Hitachi fluorescence spectrometer (F4500). Emission quantum yields were obtained by standard method<sup>10</sup> using Coumarin 1 as the reference. Cyclic voltammetry experiments were performed with a BAS-100 electrochemical analyzer. All measurements were carried out at room temperature with a conventional three-electrode configuration consisting of a glassy carbon working electrode, platinum auxiliary electrode and a nonaqueous Ag/AgNO<sub>3</sub> reference electrode. The E<sub>1/2</sub> values were determined as (E<sub>p</sub><sup>a</sup> + E<sub>p</sub><sup>c</sup>)/2, where E<sub>p</sub><sup>a</sup> and E<sub>p</sub><sup>c</sup> are the anodic and cathodic peak potentials, respectively. The solvent in all experiments was CH<sub>2</sub>Cl<sub>2</sub>, and the supporting electrolyte was 0.1 M tetrabutylammonium hexafluorophosphate. Differential scanning calorimetry (DSC) measurements were carried out on a Perkin-Elmer differential scanning calorimeter at a heating rate of 10 K/min and a cooling rate of 30 K/min under nitrogen atmosphere. Thermogravimetric analysis (TGA) measurements were performed on a TA-7 series thermogravimetric analyzer at a heating rate of 10 K/min under a flow of air.

The synthetic procedures and characterization details of the quinoxaline precursors **1–6** are presented in the Supporting Information. The target compounds **7–16** were obtained by

essentially following a similar procedure employing Pd-catalyzed C–N coupling methodology. An illustrative example is given below for **7**.

**N-(4-(2-(9,9-Diethyl-9H-fluoren-2-yl)quinoxalin-3-yl)phenyl)-N-phenylnaphthalen-1-amine (7).** A mixture of 2-(4-bromophenyl)-3-(9,9-diethyl-9H-fluoren-2-yl)quinoxaline (**5**, 1.01 g, 2.0 mmol), *N*-phenylnaphthalen-1-amine (0.482 g, 2.2 mmol), sodium *tert*-butoxide (0.288 g, 3.0 mmol), Pd(dba)<sub>2</sub> (12 mg, 0.02 mmol), P(*t*-bu)<sub>3</sub> (6 mg, 0.03 mmol), and toluene (15 mL) was heated to 80 °C under nitrogen atmosphere and stirred for 8 h. After it cooled, the solution was poured into water and extracted with diethyl ether (3 × 30 mL). The combined organic extract was dried over anhydrous MgSO<sub>4</sub> and filtered. The crude product obtained by evaporation of the volatiles was adsorbed on silica gel and purified by column chromatography. The desired compound was eluted with hexane/dichloromethane (3:2) mixture. Yellow solid. Yield: 1.16 g (90%). FAB MS: *m/z* 644 (M<sup>+</sup> + H). <sup>1</sup>H NMR (CDCl<sub>3</sub>): δ 0.28 (t, *J* = 7.3 Hz, 6 H), 1.79–1.98 (m, 4 H), 6.89–7.08 (m, 3 H), 7.09 (d, *J* = 7.7 Hz, 2 H), 7.20–7.22 (m, 2 H), 7.32–7.45 (m, 10 H), 7.73–7.93 (m, 8 H), 8.16 (br s, 2 H). Anal. Calcd for C<sub>47</sub>H<sub>37</sub>N<sub>3</sub>: C, 87.68; H, 5.79; N, 6.53. Found: C, 87.62; H, 5.64; N, 6.42.

**N-(4-(2-(9,9-Diethyl-9H-fluoren-2-yl)quinoxalin-3-yl)phenyl)-N-phenylphenanthren-9-amine (8).** Yellow solid. Yield: 76%. FAB MS: *m/z* 693 (M<sup>+</sup>). <sup>1</sup>H NMR (CDCl<sub>3</sub>): δ 0.18 (t, *J* = 7.3 Hz, 6 H), 1.76–1.99 (m, 4 H), 6.93–6.99 (m, 3 H), 7.12–7.22 (m, 4 H), 7.28–7.35 (m, 4 H), 7.39–7.64 (m, 7 H), 7.69–7.83 (m, 6 H), 7.98 (d, *J* = 8.1 Hz, 1 H), 8.13–8.18 (m, 2 H), 8.64 (d, *J* = 8.1 Hz, 1 H), 8.69 (d, *J* = 8.1 Hz, 1 H). Anal. Calcd for C<sub>51</sub>H<sub>39</sub>N<sub>3</sub>: C, 88.28; H, 5.67; N, 6.06. Found: C, 88.07; H, 5.59; N, 5.94.

**9,9-Diethyl-N-(4-(2-(9,9-diethyl-9H-fluoren-2-yl)quinoxalin-3-yl)phenyl)-N-phenyl-9H-fluoren-2-amine (9).** Yellow solid. Yield: 86%. FAB MS: *m/z* 737 (M<sup>+</sup>). <sup>1</sup>H NMR (CDCl<sub>3</sub>): δ 0.27–0.33 (m, 12 H), 1.73–2.03 (m, 8 H), 7.00–7.06 (m, 4 H), 7.11–7.15 (m, 3 H), 7.22–7.39 (m, 9 H), 7.46 (d, *J* = 8.6 Hz, 2 H), 7.55–7.62 (m, 2 H), 7.73–7.84 (m, 5 H), 8.16–8.20 (m, 2 H). Anal. Calcd for C<sub>54</sub>H<sub>47</sub>N<sub>3</sub>: C, 87.89; H, 6.42; N, 5.69. Found: C, 87.78; H, 6.37; N, 5.61.

**N-(4-(2-(9,9-Diethyl-9H-fluoren-2-yl)quinoxalin-3-yl)phenyl)-N-phenylanthracen-10-amine (10).** Yellow solid. Yield: 82%. FAB MS: *m/z* 693 (M<sup>+</sup>). <sup>1</sup>H NMR (CDCl<sub>3</sub>): δ 0.45 (t, *J* = 7.3 Hz, 6 H), 1.63–1.87 (m, 4 H), 6.85–6.90 (m, 1 H), 6.93–6.97 (m, 2 H), 7.06–7.16 (m, 4 H), 7.25–7.44 (m, 10 H), 7.67–7.74 (m, 4 H), 7.82 (dd, *J* = 8.1, 2.1 Hz, 1 H), 7.99–8.07 (m, 4 H), 8.11–8.16 (m, 2 H), 8.45 (s, 1 H). Anal. Calcd for C<sub>51</sub>H<sub>39</sub>N<sub>3</sub>: C, 88.28; H, 5.67; N, 6.06. Found: C, 88.11; H, 5.62; N, 5.87.

**N-(4-(2-(9,9-Diethyl-9H-fluoren-2-yl)quinoxalin-3-yl)phenyl)-N-phenylpyren-1-amine (11).** Yellow solid. Yield: 79%. FAB MS: *m/z* 717 (M<sup>+</sup>). <sup>1</sup>H NMR (CDCl<sub>3</sub>): δ 0.21 (t, *J* = 7.3 Hz, 6 H), 1.78–1.94 (m, 4 H), 6.92–6.99 (m, 3 H), 7.12 (d, *J* = 8.1 Hz, 2 H), 7.17–7.28 (m, 2 H), 7.26–7.32 (m, 4 H), 7.42 (d, *J* = 8.1 Hz, 2 H), 7.67–7.82 (m, 6 H), 7.92 (d, *J* = 8.1 Hz, 1 H), 7.97–8.05 (m, 3 H), 8.08–8.17 (m, 6 H). Anal. Calcd for C<sub>53</sub>H<sub>39</sub>N<sub>3</sub>: C, 88.67; H, 5.48; N, 5.85. Found: C, 88.64; H, 5.37; N, 5.70.

**N-(4-(2-(9-Ethyl-9H-carbazol-3-yl)quinoxalin-3-yl)phenyl)-N-phenylnaphthalen-1-amine (12).** Yellow solid. Yield: 78%. FAB MS: *m/z* 617 (M<sup>+</sup>). <sup>1</sup>H NMR (CDCl<sub>3</sub>): δ 1.44 (t, *J* = 7.3 Hz, 3 H), 4.36 (q, *J* = 7.3 Hz, 2 H), 6.87–6.91 (m, 3 H), 7.02–7.11 (m, 4 H), 7.24–7.53 (m, 10 H), 7.70–7.74 (m, 4 H), 7.82–7.90 (m, 2 H), 8.04 (d, *J* = 7.6 Hz, 1 H), 8.14–8.19 (m, 2 H), 8.29 (s, 1 H). Anal. Calcd for C<sub>44</sub>H<sub>32</sub>N<sub>4</sub>: C, 85.69; H, 5.23; N, 9.08. Found: C, 85.62; H, 5.17; N, 9.01.

(9) (a) Justin Thomas, K. R.; Lin, J. T.; Tao, Y.-T.; Ko, C.-W. *Adv. Mater.* **2000**, *12*, 1949. (b) Justin Thomas, K. R.; Lin, J. T.; Tao, Y.-T.; Ko, C.-W. *J. Am. Chem. Soc.* **2001**, *123*, 9404.  
(10) Demas, J. N.; Crosby, G. A. *J. Phys. Chem.* **1971**, *75*, 991.

***N*-(4-(2-(9-Ethyl-9*H*-carbazol-3-yl)quinoxalin-3-yl)phenyl)-*N*-phenylphenanthren-9-amine (13).** Yellow solid. Yield: 79%. FAB MS:  $m/z$  666 ( $M^+$ ).  $^1\text{H}$  NMR ( $\text{CDCl}_3$ ):  $\delta$  1.43 (t,  $J = 7.3$  Hz, 3 H), 4.35 (q,  $J = 7.3$  Hz, 2 H), 6.90–6.96 (m, 3 H), 7.06–7.17 (m, 4 H), 7.25–7.48 (m, 6 H), 7.50–7.53 (m, 3 H), 7.56–7.65 (m, 3 H), 7.70–7.75 (m, 3 H), 7.97 (d,  $J = 7.6$  Hz, 1 H), 8.02 (d,  $J = 7.6$  Hz, 1 H), 8.14–8.19 (m, 2 H), 8.17 (d,  $J = 2.1$  Hz, 1 H), 8.62 (d,  $J = 8.1$  Hz, 1 H), 8.68 (d,  $J = 8.1$  Hz, 1 H). Anal. Calcd for  $\text{C}_{48}\text{H}_{34}\text{N}_4$ : C, 86.46; H, 5.14; N, 8.40. Found: C, 86.40; H, 5.03; N, 8.22.

**9,9-Diethyl-*N*-(4-(2-(9-ethyl-9*H*-carbazol-3-yl)quinoxalin-3-yl)phenyl)-*N*-phenyl-9*H*-fluoren-2-amine (14).** Orange solid. Yield: 83%. FAB MS:  $m/z$  711 ( $M^+ + \text{H}$ ).  $^1\text{H}$  NMR ( $\text{CDCl}_3$ ):  $\delta$  0.28 (t,  $J = 7.3$  Hz, 6 H), 1.47 (t,  $J = 7.3$  Hz, 3 H), 1.71–1.92 (m, 4 H), 4.39 (q,  $J = 7.3$  Hz, 4 H), 6.95–7.17 (m, 9 H), 7.20–7.31 (m, 4 H), 7.41–7.58 (m, 7 H), 7.71–7.76 (m, 2 H), 7.85 (dd,  $J = 8.8$ , 1.6 Hz, 1 H), 8.05 (d,  $J = 7.6$  Hz, 1 H), 8.16–8.22 (m, 2 H), 8.23 (d,  $J = 1.6$  Hz, 1 H). Anal. Calcd for  $\text{C}_{51}\text{H}_{42}\text{N}_4$ : C, 86.16; H, 5.95; N, 7.88. Found: C, 86.02; H, 5.81; N, 7.71.

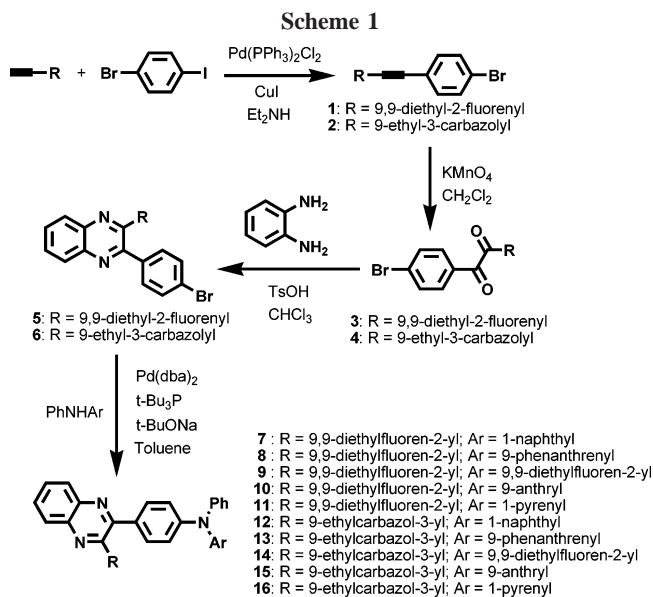
***N*-(4-(2-(9-Ethyl-9*H*-carbazol-3-yl)quinoxalin-3-yl)phenyl)-*N*-phenylanthracen-10-amine (15).** Yellow solid. Yield: 94%. FAB MS:  $m/z$  666 ( $M^+$ ).  $^1\text{H}$  NMR ( $\text{CDCl}_3$ ):  $\delta$  1.42 ( $J = 7.3$  Hz, 3 H), 4.34 (q,  $J = 7.3$  Hz, 2 H), 6.81–6.91 (m, 3 H), 7.02–7.09 (m, 4 H), 7.22–7.5 (m, 10 H), 7.63 (dd,  $J = 8.8$ , 2.1 Hz, 1 H), 7.67–7.73 (m, 2 H), 7.99–8.05 (m, 5 H), 8.11–8.19 (m, 2 H), 8.29 (d,  $J = 2.1$  Hz, 1 H), 8.46 (s, 1 H). Anal. Calcd for  $\text{C}_{48}\text{H}_{34}\text{N}_4$ : C, 86.46; H, 5.14; N, 8.40. Found: C, 86.34; H, 5.09; N, 8.37.

***N*-(4-(2-(9-Ethyl-9*H*-carbazol-3-yl)quinoxalin-3-yl)phenyl)-*N*-phenylpyren-1-amine (16).** Yellow solid. Yield: 86%. FAB MS:  $m/z$  691 ( $M^+ + \text{H}$ ).  $^1\text{H}$  NMR ( $\text{CDCl}_3$ ):  $\delta$  1.34 (t,  $J = 7.3$  Hz, 3 H), 4.26 (q,  $J = 7.3$  Hz, 2 H), 6.88–6.97 (m, 3 H), 7.06–7.16 (m, 4 H), 7.29 (t,  $J = 6.7$  Hz, 2 H), 7.37–7.43 (m, 3 H), 7.49–7.52 (m, 1 H), 7.69–7.79 (m, 5 H), 7.94–8.06 (m, 7 H), 8.14 (dd,  $J = 8.1$ , 2.1 Hz, 1 H), 8.18–8.22 (m, 2 H), 8.26 (d,  $J = 2.1$  Hz, 1 H). Anal. Calcd for  $\text{C}_{50}\text{H}_{34}\text{N}_4$ : C, 86.93; H, 4.96; N, 8.11. Found: C, 86.79; H, 4.81; N, 7.96.

**OLED Fabrication and Measurements.** Electron-transporting materials TPBI (1,3,5-tris(*N*-phenylbenzimidazol-2-yl)-benzene)<sup>11</sup> and Alq<sub>3</sub> (tris(8-hydroxyquinolino)aluminum)<sup>12</sup> were synthesized according to literature procedures and were sublimed twice prior to use. Prepatterned indium–tin oxide (ITO) substrates with an effective individual device area of 3.14 mm<sup>2</sup> were cleaned as described in a previous report.<sup>13</sup> Double-layer electroluminescence (EL) devices using quinoxaline derivatives (**7**–**16**) as the hole-transport layer and TPBI or Alq<sub>3</sub> as the electron-transport layer were fabricated. For comparison, a typical device using NPB (4,4'-bis(1-naphthylphenylamino)biphenyl) as the hole-transporting layer was also prepared. All devices were prepared by vacuum depositing 400 Å of the hole-transporting layer (compounds **7**–**16**), followed by 400 Å of TPBI or Alq<sub>3</sub>. An alloy of magnesium and silver (ca. 10:1, 500 Å) was deposited as the cathode, which was capped with 1000 Å of silver. The *I*-*V* curve was measured on a Keithley 2400 Source Meter in an ambient environment. Light intensity was measured with a Newport 1835 Optical Meter.

## Results and Discussion

**Synthesis and Characterization.** The syntheses of the quinoxaline–triarylamine dyads (**7**–**16**) containing additional



chromophores such as carbazole, fluorene, and pyrene were achieved in four steps (Scheme 1). The first three steps (Sonogashira coupling<sup>14</sup> of the corresponding terminal acetylene with 1-bromo-4-iodobenzene, oxidation of diketones to  $\alpha,\beta$ -diketones, and the condensation of diketones with *o*-phenylene diamine) led to the desired bromophenylquinoxaline precursors (**5** and **6**). These intermediates were later converted to the target compounds by the palladium catalyzed C–N coupling reactions<sup>15</sup> involving Pd-(dba)<sub>2</sub>/P(*t*-Bu)<sub>3</sub> catalyst and *t*-BuONa base. The compounds are intense yellow or orange in color and are soluble in most organic solvents but insoluble in alcohols. The  $^1\text{H}$  NMR recorded in  $\text{CDCl}_3$ , mass spectral, and elemental analyses data are in accordance with the structure of the molecules.

**Photophysical Properties.** The linear optical properties of the compounds were examined both by absorption and emission spectroscopy. The optical data are compiled in Table 1. In the absorption spectra, all the compounds displayed a band located at ca. 400 nm possibly originating from the charge-transfer (CT) transition. Additional peaks attributable to the  $\pi$ – $\pi^*$  transition of the chromophores such as fluorene, pyrene, and carbazole were also noticed around the 320-nm region in the compounds containing those functional moieties. The CT band does not display any trend due to the presence of chromophores. They are not affected by the solvent of measurement, either. On the contrary, the emission spectra of the compounds are sensitive to the chromophores (Figure 1) and the polarity of the solvent (Figure 2). Presence of chromophore on the triarylamine unit affects the emission maxima significantly. For a given quinoxaline structure, the triarylamine's influence on the wavelength of the emission maximum is manifested in the following order: naphthalene  $\approx$  phenanthrene < anthracene

- (11) (a) Shi, J.; Tang, C. W.; Chen, C. H. U.S. Patent 5,645,948, 1997. (b) Sonsale, A. Y.; Gopinathan, S.; Gopinathan, C. *Ind. J. Chem.* **1976**, *14*, 408.  
(12) Chen, C. H.; Shi, J.; Tang, C. W. *Coord. Chem. Rev.* **1998**, *171*, 161.  
(13) Justin Thomas, K. R.; Lin, J. T.; Velusamy, M.; Tao, Y. T.; Chuen, C. H. *Adv. Funct. Mater.* **2004**, *14*, 83.

- (14) (a) Sonogashira, K.; Tohda, Y.; Hagihara, N. *Tetrahedron Lett.* **1975**, 4467–4470. (b) Hundertmark, T.; Littke, A. F.; Buchwald, S. L.; Fu, G. C. *Org. Lett.* **2000**, *2*, 1729–1731.  
(15) (a) Hartwig, J. F. *Synlett* **1997**, 329. (b) Hartwig, J. F. *Angew. Chem., Int. Ed. Engl.* **1998**, *37*, 2046. (c) Hartwig, J. F. *Acc. Chem. Res.* **1998**, *31*, 852–860. (d) Hartwig, J. F.; Kawatsura, M.; Hauck, S. I.; Shaughnessy, K. H.; Alcazar-Roman, L. M. *J. Org. Chem.* **1999**, *64*, 5575.



Table 1. Photophysical, Thermal, and Redox Properties for the Compounds

compd	$\lambda_{\text{abs}}$ , nm		$\lambda_{\text{em}}$ , nm ( $\Phi_f$ , %)		$T_g$ , °C	$T_d$ , °C	$E_{\text{ox}}$ ( $\Delta E_p$ ), mV	$E_{\text{red}}$ ( $\Delta E_p$ ), mV	HOMO, eV	LUMO, eV
	toluene	CH <sub>2</sub> Cl <sub>2</sub>	toluene	CH <sub>2</sub> Cl <sub>2</sub>						
7	316, 397	284, 315, 398	480 (8)	547 (11)	102	396	611 (64)	−2147 (90)	5.41	2.65
8	317, 394	277, 317, 394	478 (28)	544 (21)	126	420	648 (161)	−2132 (i)	5.45	2.63
9	324, 405	290, 335, 407	500 (11)	589 (3)	104	399	441 (67)	−2152 (90)	5.24	2.65
10	317, 402	283, 317, 399	490 (26)	528 (20)	130	415	587 (110)	−2148 (i)	5.39	2.63
11	316, 404	275, 317, 401	490 (34)	574 (5)	125	410	499 (66)	−2151 (105)	5.30	2.54
12	400	287, 398	477 (11)	538 (18)	111	406	570 (84)	−2171 (122)	5.37	2.64
13	316, 398	280, 317, 400	475 (27)	539 (29)	138	440	638 (60)	−2220 (i)	5.44	2.65
14	334, 405	290, 332, 407	497 (13)	582 (6)	117	415	421 (70)	−2171 (122)	5.22	2.63
15	319, 405	284, 320, 403	496 (22)	520 (45)	143	440	548 (73)	−2184 (i)	5.35	2.62
16	315, 408	275, 317, 402	484 (34)	567 (10)	146	425	493 (60)	−2196 (i)	5.29	2.54

$\approx$  pyrene < fluorene when recorded in toluene.<sup>9b</sup> For example, the emission profile in toluene for the fluorenyl-quinoxalines adopt the order: **7**  $\approx$  **8** < **10**  $\approx$  **11** ( $\Delta\lambda = 10$  nm) < **9** ( $\Delta\lambda = 20$  nm). Triaryl amines showing emission features due to the chromophores attached to it is well documented in the literature.<sup>16</sup> Chromophores on the quinoxaline unit have a less-pronounced effect on the emission maxima. The magnitude of solvatochromic emission shift is small for anthracenylamine derivatives and larger for pyrenyl and fluorenylamine derivatives (see for instance

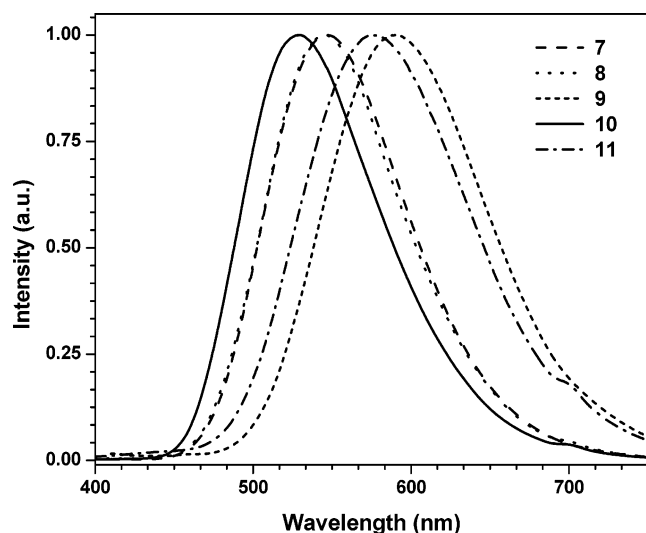


Figure 1. Emission spectra of the fluorenylquinoxaline derivatives (7–11) recorded in dichloromethane solution.

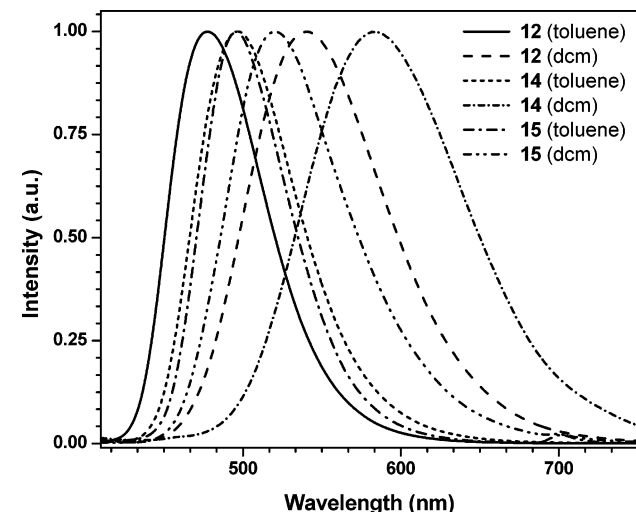


Figure 2. Illustrative examples of solvent effect observed in emission spectra.

Figure 2). Pyrenyl and fluorenylamine derivatives show diminished quantum yield when recorded in dichloromethane solutions. Anthracenyl and phenanthrenylamines result in moderate quantum yields in both toluene and dichloromethane solutions. It is believed that the trends observed in quantum yield and solvent dependence of the emission are mainly dictated by the decay processes due to oxidative quenching of the amines.<sup>17</sup> Such nonradiative decay processes will be more pronounced in polar solvents when compared to the apolar solvents. This assumption is reasonable as most of the compounds that display comparatively lower oxidation potentials (vide infra) exhibit less quantum efficiency when recorded in polar solvents. Interestingly, the molecules reported here exhibit emission at lower wavelength when compared to the related quinoxaline derivatives that contain bis(diaryl amino) arms.<sup>5b</sup> The later compounds possibly possess larger molecular dipole owing to the presence of two donor segments and leads to red-shifted absorption and emission profiles.

**Thermal Properties.** The thermal stability and the amorphous nature of the compounds were investigated by thermogravimetry and differential scanning calorimetry, respectively. All the compounds show glass transition temperatures higher than those observed for the commonly used hole-transporting agents TPD (*N,N'*-diphenyl-*N,N'*-bis(3-methylphenyl)-1,1'-biphenyl-4,4'-diamine) and NPB (4,4'-bis(1-naphthylphenylamino)biphenyl). The glass transition temperature increases progressively on incorporating the chromophores such as pyrene, anthracene, and carbazole. Thus, the compounds **16** and **15** exhibit the highest  $T_g$  among the present series. The decomposition temperatures of the compounds are generally higher than 350 °C. The carbazole derivatives (**12**–**16**) possess elevated decomposition temperatures when compared to the corresponding fluorene analogues (**7**–**11**). The role of carbazole on increasing the glass transition temperature and thermal stability is well witnessed in the literature.<sup>9,18</sup>

**Electrochemical Properties.** The redox propensity of the compounds was estimated by measuring the cyclic voltam-

- (16) Hreha, R. D.; George, C. P.; Haldi, A.; Domercq, B.; Malagoli, M.; Barlow, S.; Bredas, J. L.; Kippelen, B.; Marder, S. R. *Adv. Funct. Mater.* **2003**, *13*, 967.
- (17) (a) Castner, E. W.; Kennedy, D.; Cave, R. J. *J. Phys. Chem. A* **2000**, *104*, 2869. (b) Hilczler, M.; Traytak, S.; Tachiya, M. *J. Chem. Phys.* **2001**, *115*, 11249.
- (18) (a) Kundu, P.; Justin Thomas, K. R.; Lin, J. T.; Tao, Y.-T.; Chien, C. H. *Adv. Funct. Mater.* **2003**, *13*, 445. (b) Grazulevicius, J. V.; Strohmriegel, P.; Pielichowski, J.; Pielichowski, K. *Prog. Polym. Sci.* **2003**, *28*, 1297.

Table 2. Electroluminescent Data for the Compounds

	7	8	9	10	11	12
			TPBI/Alq <sub>3</sub>			
turn-on voltage, V	3.5/3.0	3.5/3.0	3.5/3.5	3.5/3.0	3.5/3.0	3.5/3.0
max. brightness, cd/m <sup>2</sup>	16920/12920	30860/23320	35160/40390	27840/21160	49120/41690	31390/37630
max. ext. quantum eff., %	1.43/0.77	1.50/1.00	2.12/2.08	1.75/0.89	1.58/1.54	2.47/1.83
max. power eff., lm/W	2.44/1.43	1.76/1.77	3.93/3.31	3.48/1.54	2.22/2.85	3.69/2.89
max. current eff., cd/A	3.50/2.30	3.44/2.89	6.37/6.63	4.43/2.71	4.73/4.86	6.98/5.59
$\lambda_{\text{film}}$ (fwhm), nm	498 (70)	504 (82)	514 (72)	502 (68)	514 (74)	508 (76)
$\lambda_{\text{EL}}$ (fwhm), nm	496 (68)/510 (88)	490 (68)/502 (88)	506 (68)/514 (78)	496 (62)/504 (80)	504 (66)/510 (76)	500 (72)/502 (76)
CIE, x, y	0.16, 0.44/0.26, 0.52	0.16, 0.38/0.23, 0.48	0.21, 0.54/0.28, 0.56	0.16, 0.45/0.24, 0.52	0.20, 0.53/0.24, 0.54	0.19, 0.50/0.23, 0.53
voltage, <sup>a</sup> V	6.98/6.86	6.62/5.51	7.15/7.17	6.21/6.00	6.56/5.27	7.86/6.65
brightness, <sup>a</sup> cd/m <sup>2</sup>	2960/2385	3420/2850	5960/6600	3610/2600	4570/4670	6760/5560
ext. quantum eff., <sup>a</sup> %	1.21/0.77	1.50/0.98	2.00/2.08	1.44/0.85	1.53/1.48	2.40/1.82
power eff., <sup>a</sup> lm/W	1.33/1.09	1.63/1.63	2.63/2.90	1.84/1.36	2.19/2.78	2.71/2.63
current eff., <sup>a</sup> cd/A	2.97/2.38	3.43/2.85	5.98/6.61	3.63/2.60	4.57/4.65	6.77/5.56
	13	14	15	16		
		TPBI/Alq <sub>3</sub>				
turn-on voltage, V	3.5/3.0	3.0/3.0	3.5/2.5	3.5/3.0		
max. brightness, cd/m <sup>2</sup>	14370/26000	61800/61460	39430/37050	70850/61620		
max. ext. quantum eff., %	1.14/1.06	2.69/2.24	1.43/1.23	2.04/1.27		
max. power eff., lm/W	1.49/1.82	5.13/4.31	2.31/1.96	3.14/1.61		
max. current eff., cd/A	3.17/3.18	8.80/7.64	4.57/4.00	6.65/4.22		
$\lambda_{\text{film}}$ (fwhm), nm	508 (72)	522 (78)	518 (74)	528 (82)		
$\lambda_{\text{EL}}$ (fwhm), nm	502 (68)/512 (86)	514 (70)/518 (76)	510 (70)/512 (76)	512 (72)/514 (76)		
CIE, x, y	0.20, 0.51/0.26, 0.53	0.25, 0.58/0.27, 0.59	0.22, 0.57/0.25, 0.57	0.23, 0.57/0.25, 0.57		
voltage, <sup>a</sup> V	8.34/6.16	7.02/6.64	6.23/4.82	6.18/3.36		
brightness, <sup>a</sup> cd/m <sup>2</sup>	2980/3160	8220/7640	4480/1530	6180/130		
ext. quantum eff., <sup>a</sup> %	1.07/1.06	2.52/2.24	1.40/0.46	1.88/0.04		
power eff., <sup>a</sup> lm/W	1.13/1.60	3.68/3.62	2.26/0.97	3.13/0.11		
current eff., <sup>a</sup> cd/A	2.99/3.16	8.23/7.64	4.47/1.51	6.15/0.12		

<sup>a</sup> At a current density of 100 mA/cm<sup>2</sup>.

mograms in dichloromethane solutions. All the compounds displayed a quasi-reversible oxidation couple and a reduction wave. The reduction wave due to the quinoxaline unit predominantly remains irreversible except for the few compounds (**7**, **9**, and **11**). The oxidation potential is sensitive to the triarylamine chromophores. Thus, for a given quinoxaline series, the oxidation potential assumes the following order with respect to the triarylamine unit: phenanthrene > naphthalene > anthracene > pyrene > fluorene. Earlier fluorenylamines were found to possess lower oxidation potential when compared to the biphenyl analogues.<sup>19</sup> It is interesting to note that the additional chromophores attached to the quinoxaline nucleus do not exert any significant effect on the reduction potential of the quinoxaline segment.

**Electroluminescent Devices.** The oxidation potential and the absorption edge from the photophysical data were utilized to obtain the highest-occupied molecular orbital (HOMO) and lowest-unoccupied molecular orbital (LUMO) energy levels, respectively, using ferrocene (4.8 eV) as a standard. Inspection of these values for the present compounds suggests that they may be capable of transporting both holes and electrons. Though the compounds all have LUMOs lying close to TPBI (2.70 eV) which reduces the energy barrier for electron injection, they failed to produce intense emission when applied as a single layer or the electron-transporting/emitting layer. On the contrary, when the compounds were applied as hole-transport layer in conjunction with the electron-transport materials (TPBI/Alq<sub>3</sub>), in LEDs, they produced intense emission (Table 2). This clearly identifies

that the electron injection/transport capabilities of these compounds are still limited.

As mentioned above, two sets of devices were made for each compound varying the electron-transport layer from TPBI to Alq<sub>3</sub>. All the devices lead to intense emission. The emission color of the devices may be broadly described as green. A representative EL and photoluminescence (PL) comparison for compound **14** is provided in Figure 3. The

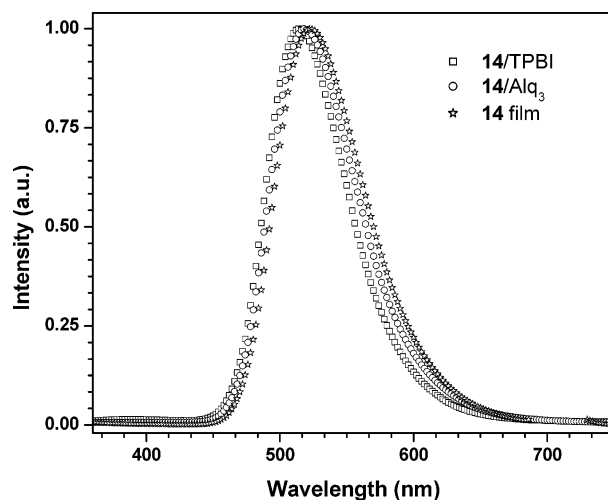


Figure 3. PL and EL comparison for compound **14**.

emission appears to be resulting from the compounds in most devices. However, close inspection reveals that all the Alq<sub>3</sub> devices display slightly broad and red-tailing emission profiles when compared to those of TPBI-based devices and film PL. This suggests that there is a contribution from the Alq<sub>3</sub> emission in those devices. This is probably a result of

(19) Loy, D. E.; Koene, B. E.; Thompson, M. E. *Adv. Funct. Mater.* **2002**, *12*, 245.

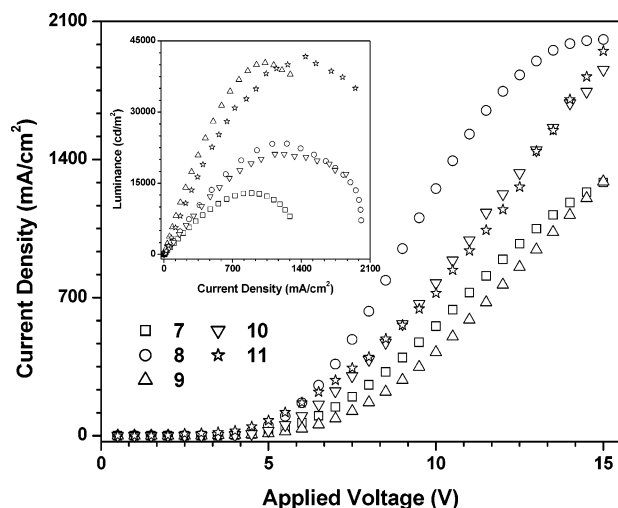


Figure 4.  $I$ - $V$ - $L$  characteristics for the  $\text{Alq}_3$ -based devices with hole-transporting quinoxalines, 7–11.

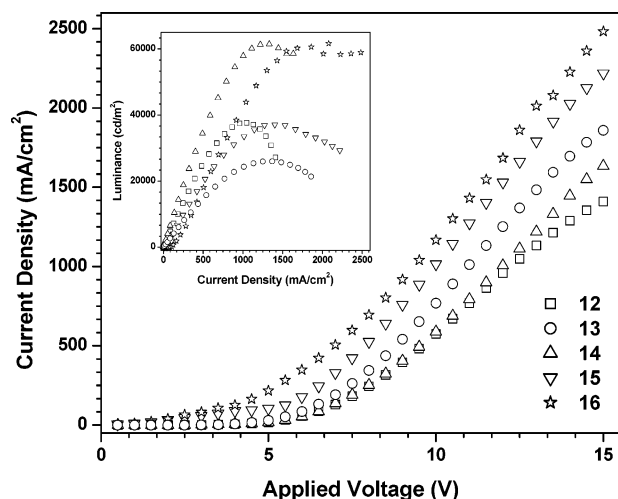


Figure 5.  $I$ - $V$ - $L$  characteristics for the  $\text{Alq}_3$ -based devices with hole-transporting quinoxalines, 12–16.

a recombination zone located close to the interface of HTL/ $\text{Alq}_3$  (HTL = hole-transport layer;  $\text{Alq}_3$  = tris(8-hydroxy-quinolino) aluminum). Additionally, a slight blue shift in the EL spectra was noticed for the most devices when compared to the PL spectra of the vapor-deposited pure films. This may be due to the microstructure variation between the pure film and the device.<sup>20</sup>

The device characteristics of the compounds are displayed in Figures 4–7, and the corresponding parameters are listed in Table 2. Among the devices, those containing pyrenyl, anthryl, and phenanthrenylamines (compounds 8, 10, 11, 13, 15, and 16) display larger current densities at higher voltages. We speculate that in these compounds the planar and rigid aromatic moieties (pyrene, anthracene, and phenanthrene) present in the triarylamine segment facilitate the hole-hopping process through intermolecular interactions.<sup>21</sup> In general, most of the compounds show promising performance in terms of brightness and external quantum efficiency. Green emitting devices of the compounds 11, 14, and 16 show exceptional brightness. Table 3 presents a comparison of

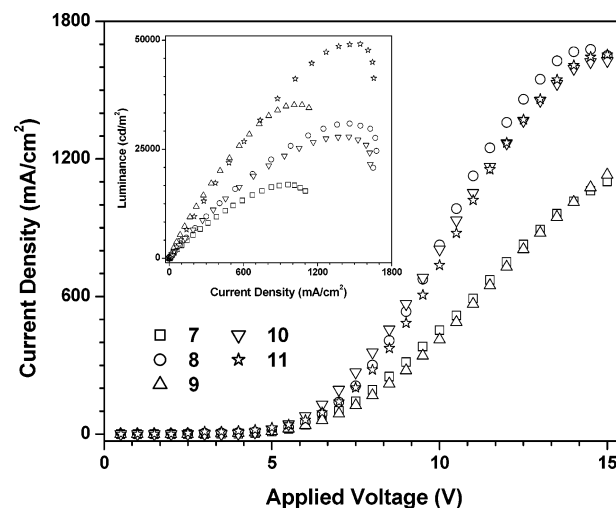


Figure 6.  $I$ - $V$ - $L$  characteristics for the TPBI-based devices with hole-transporting quinoxalines, 7–11.

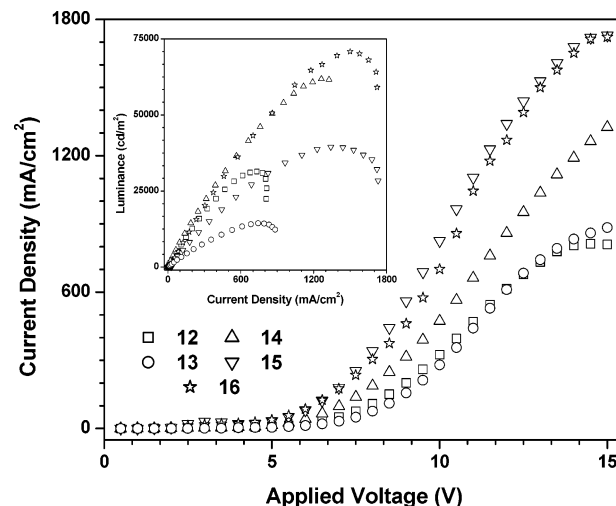


Figure 7.  $I$ - $V$ - $L$  characteristics for the TPBI-based devices with hole-transporting quinoxalines, 12–16.

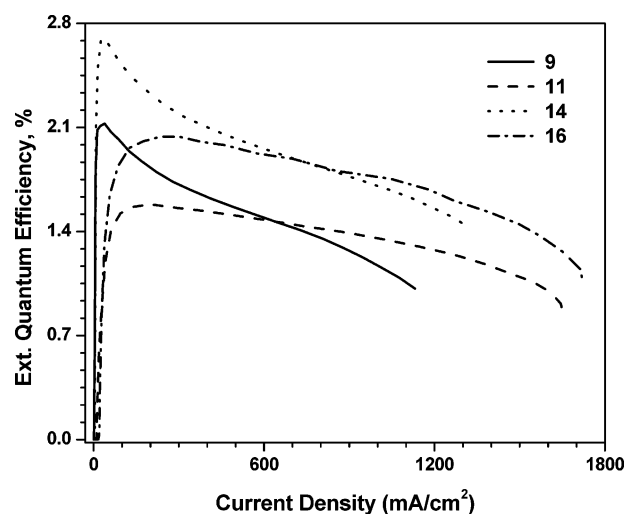


Figure 8. Variation of external quantum efficiency observed for selected TPBI based devices with operating voltage.

device performance for the known compounds in the literature along with the promising compounds 11, 14, and 16. It is evident that, among the unoptimized devices,

(20) Dirr, S.; Wiese, S.; Johannes, H.-H.; Kowalsky, W. *Adv. Mater.* **1998**, *10*, 167.

Table 3. Comparison of Selected Green Emitting Devices

compound, device	$\lambda_{\text{em}}$ , nm/CIE (x, y)	$L$ , <sup>a</sup> cd/m <sup>2</sup>	$\eta_{\text{ext}}$ , <sup>a</sup> %	$\eta_{\text{p}}$ , <sup>a</sup> lm/W	$L_{\text{max}}$ , cd/m <sup>2</sup>	ref
2,3-Bis[4-( <i>N</i> -phenyl-naphthylamino)phenyl]quinoxaline, ITO/X/TPBI/Mg:Ag	492/0.16, 0.41;	3829	1.63	1.86	25370	5b
Tris(quinolinato)Aluminum(III), ITO/ $\alpha$ -NPB/X/Mg:Ag	520	2870	1.07	1.42	30200	22
9,10-Bis(1-naphthylphenylamino)anthracene, ITO/ <i>m</i> -MTDATA(20 nm)/X(40 nm)/TPBI(50 nm)/Mg:Ag	522/0.24, 0.69	11150	2.86	4.25	65120	23
4-(3-( <i>N</i> -phenyl- <i>N</i> -(pyren-1-yl)amino)-6-( <i>N</i> -phenyl- <i>N</i> -(pyren-8-yl)amino)-9 <i>H</i> -carbazol-9-yl)benzonitrile, ITO/X/TPBI/Mg:Ag	500/0.22, 0.47	5362	2.10	3.26	48200	9b
<b>11</b> , ITO/X/TPBI/Mg:Ag	504/0.20, 0.53	4570	1.53	2.19	49120	this work
<b>14</b> , ITO/X/TPBI/Mg:Ag	514/0.25, 0.58	8220	2.53	3.68	61800	this work
<b>16</b> , ITO/X/TPBI/Mg:Ag	512/0.23, 0.57	6180	1.88	3.13	70850	this work

<sup>a</sup> At a current density of 100 mA/cm<sup>2</sup>.

compounds **11**, **14**, and **16** show promising parameters and better than the standard green emitting ITO/ $\alpha$ -NPB/Alq<sub>3</sub>/Mg:Ag device.<sup>22</sup> It is to be noted that the exceptional performance realized for the compound 9,10-bis(1-naphthylphenylamino)anthracene is a result of a combinatorial device engineering.<sup>23</sup>

Though the unoptimized devices experience device instability at higher operating voltages (Figure 8) as evidenced by a rapid drop in the quantum efficiency at higher current densities, we believe that further device engineering can greatly improve the performance characteristics.

## Summary

We have designed and synthesized a new series of compounds that contain electron-deficient quinoxaline, electron-rich triarylamine segments, and fluorophores such as pyrene, carbazole, and fluorene. We unravel that the incorporation of fluorene and pyrene greatly improve the brightness of the emission in the devices while fragments such as carbazole and pyrene strengthen the thermal properties, viz., glass transition temperature and decomposition temperature. Combined with the high glass transition temperature, thermal stability, and good fluorescence properties, these molecules are potential candidates for electronic devices.

**Acknowledgment.** We thank Academia Sinica and the National Science Council for financial support.

**Supporting Information Available:** Synthesis and characterization details of the bromophenyl quinoxaline precursors. This material is available free of charge via the Internet at <http://pubs.acs.org>.

CM047705A

- (21) Three-layer devices with a structure of ITO/NPB (40 nm)/**9**, **11**, or **16** (10 nm)/TPBI or Alq<sub>3</sub> (30 nm)/Mg:Ag (NPB = 1,4-bis[(1-naphthylphenyl)amino]biphenyl) were fabricated. All these three devices display similar current density, and the current density of these devices for **11** and **16** was slightly higher than that of the double-layer devices. These observations suggest that **11** and **16** have greater hole mobility than **9**.
- (22) Ko, C. W.; Tao, Y. T. *Synth. Met.* **2002**, *126*, 37.
- (23) Yu, M.-X.; Duan, J.-P.; Lin, C.-H.; Cheng, C.-H.; Tao, Y.-T. *Chem. Mater.* **2002**, *14*, 3958.